A study of the ANNNI model using a dissipative map

1996 J. Phys.: Condens. Matter 8 5325

(http://iopscience.iop.org/0953-8984/8/29/009)

J. Phys.: Condens. Matter **8** (1996) 5325–5344. Printed in the UK

A study of the ANNNI model using a dissipative map

Jaichul Yi, G S Canright and I M Sandler

Department of Physics and Astronomy, University of Tennessee, Knoxville, TN 37996-1200, and Solid State Division, Oak Ridge National Laboratory, Oak Ridge, TN 37831, USA

Received 23 February 1996

Abstract. It is well known that extrema of classical, one-dimensional systems can be viewed as trajectories of a nonlinear, volume-preserving map. However, in general, thermodynamically stable extrema (i.e., local minima) of the free energy are numerically unstable trajectories of the map and so difficult to study by this technique. Here we explore a recent idea involving the use of a *dissipative* map to study the same kind of problem. Such a map may be designed so that its attractors are equal to, or close to, local minima of the energy. We apply such a dissipative map to the mean-field ANNNI model. We find that the technique reliably locates many kinds of metastable state: ferromagnetic, paramagnetic, commensurate, and incommensurate. However, the map also has two notable failings: it (apparently) has no chaotic attractors; and it fails to find correctly metastable states in a region of the phase diagram which is dominated by incommensurate states.

1. Introduction

Frustrated systems are of interest due to the rich variety of stable and metastable structures to which they give rise. One-dimensional frustrated systems are particularly well-studied. One idea that has been much used for 1D systems [1–6] is to write the N equations (N being the length of the chain) for extremizing the free energy $F(\{M_i\})$ (a function of the 'spins' M_i) as an iterated nonlinear map $\mathcal{M}_v$. Here the subscript v reminds us [7] that such a map is volume-preserving. Two other features of the map $\mathcal{M}_v$ are worth noting. One is that, for interactions of (integer) range r, $\mathcal{M}_v$ is $2r$-dimensional. Another is that the *numerical* or *mapping* stability of trajectories of $\mathcal{M}_v$ is anticorrelated [1, 2, 5] with the *thermodynamic* stability of the corresponding extrema. That is, trajectories which are readily accessible numerically are, almost always, physically unstable.

This problem can be avoided, at least in part, by (i) avoiding reliance on numerical trajectories, i.e., proving properties [1, 2, 4, 5] of the global or local minima of the energies as trajectories (albeit unstable) of $\mathcal{M}_v$; (ii) working with finite chains [6], so that boundary conditions allow the unique determination of the trajectory; or (iii) other means, such as determining, as narrowly as possible, numerical bounds [1, 2] for the location of the (numerically) unstable orbits of interest. All of these techniques are least useful for the *disordered* metastable states of the 1D problem, represented by chaotic trajectories of the map. There are generally good physical reasons to expect such metastable states (e.g., as irregular spacings of pinned solitons). However, the numerically stable trajectories of the map $\mathcal{M}_v$ provide little detailed information about chaotic metastable states; and the alternatives (i)–(iii) above are equally limited in their utility for such trajectories.

Recently, Watson and Canright [8] described a dissipative iterated map $\mathcal{M}_d$ which they applied to pinned flux-line lattices in layered superconductors. This problem, given

0953-8984/96/295325+20$19.50

certain assumptions, maps to a highly frustrated one-dimensional chain with the interaction range depending on a parameter. Watson and Canright found that, as the interaction range reached around 5–10 lattice spacings, chaotic metastable states appeared at low energy, in fact nearly competitive with the state of lowest known energy (which was periodic). These states were readily studied, in detail, because they appeared (approximately) as *attractors* of the dissipative map $\mathcal{M}_d$—along with other metastable states.

The idea of Watson and Canright (i.e., of using $\mathcal{M}_d$) thus appears complementary to the notion of applying a map $\mathcal{M}_v$ to study metastable states. The dissipative map possesses attractors, which are, approximately or sometimes exactly, *some of* the metastable states of the 1D problem. In contrast, the precise trajectories of the volume-preserving map $\mathcal{M}_v$ include (besides all of the unstable extrema) *all* metastable states of the problem; but these states can be difficult or impossible to extract numerically.

For these reasons, we believe that the idea of applying a dissipative iterated map to frustrated 1D problems merits further study. We report here a study of the ANNNI model at the level of mean-field theory, using a map $\mathcal{M}_d$. The ANNNI model [9] has been intensely studied, as it is one of the 'prototype' frustrated models, one which gives rise to a rich variety (in fact, an infinity) of equilibrium phases, including ferromagnetic, commensurate, incommensurate, and disordered (paramagnetic) phases. The mean-field ANNNI model has been studied by Høgh Jensen and Bak [1] using a volume-preserving map $\mathcal{M}_v$. This work exploits the map $\mathcal{M}_v$ to reach specific conclusions about the ferromagnetic/paramagnetic phase boundary, the incommensurate/commensurate transition, and soliton properties; it also strongly suggests the existence of chaotic metastable states.

In the present work, we design a dissipative map for the same problem, and study its attractors over the two-dimensional parameter space. We find that the resulting map has a rich variety of attractors which, in most regions of the parameter space, represent metastable (or stable) states of the mean-field ANNNI problem. These attractors include ferromagnetic, paramagnetic, commensurate, and incommensurate states, including periodic arrays of pinned solitons. In contrast to the results of Watson and Canright, however, we find no chaotic attractors for our map $\mathcal{M}_d$. We also find that, in a certain regime of parameter space, the map commonly generates structures which are not metastable states of the mean-field ANNNI problem.

Below, we describe our method (section 2) and results (section 3) in detail; the final section (4) then offers our conclusions.

2. The dissipative map

The mean-field free energy of the ANNNI model [9] is (with $k_B = 1$)

$$F = \frac{1}{2}T\sum_i[(1+M_i)\ln(1+M_i)+(1-M_i)\ln(1-M_i)] - 2J_0\sum_i M_i^2 - \frac{1}{2}\sum_i[J_1M_i(M_{i-1}+M_{i+1})+J_2M_i(M_{i-2}+M_{i+2})] \qquad (2.1)$$

where i is a layer index, M_i is the mean-field magnetization of layer i ($-1 \leqslant M_i \leqslant 1$), T is the temperature, J_1 and J_2 are interlayer couplings, and J_0 is the intralayer interaction. Extrema of F satisfy the following infinite set of coupled equations:

$$\frac{\partial F}{\partial M_i} = 0. \qquad (2.2)$$

From equation (2.2) one can obtain a relation of the form

$$M_{i+2} = V_F(M_{i+1}, M_i, M_{i-1}, M_{i-2}). \tag{2.3}$$

This relation, in turn, may be written as an iterated, four-dimensional map, which may be shown to be volume-preserving [1].

In contrast to this four-dimensional map, we design a two-dimensional map as follows. We define a function, $G(M_i, M_{i-1}, M_{i-2})$, resembling the free energy F of equation (2.1), by

$$G(M_i, M_{i-1}, M_{i-2}) = \frac{1}{2}g_T[(1+M_i)\ln(1+M_i) + (1-M_i)\ln(1-M_i)] \\ -g_0M_i^2 - g_1M_iM_{i-1} - g_2M_iM_{i-2} \tag{2.4}$$

where g_T, g_0, g_1 and g_2 are as-yet undetermined parameters, to be related to those in equation (2.1). Clearly, G is just the 'local' free energy of M_i, with the bonds to the right rescaled to zero (and the remaining couplings also subject to a possible rescaling). G is chosen to be completely asymmetric in this way, in order to facilitate the dynamical 'growth' of a chain from one end. That is, with the function G, we can design the dissipative map $\mathcal{M}_d$ as an iterated minimization process, as follows. Given M_{i-1} and M_{i-2}, we choose M_i to satisfy

$$G(M_i, M_{i-1}, M_{i-2}) = \min_x G(x, M_{i-1}, M_{i-2}). \tag{2.5}$$

Iteration of equation (2.5) then gives a *two*-dimensional map $\mathcal{M}_d$, with which one can 'grow' a chain of arbitrary length.

The map $\mathcal{M}_d$ represented by equations (2.4) and (2.5) is a rather simple structure, which, however, cannot be written explicitly in the form $M_i = V_G(M_{i-1}, M_{i-2})$ (which would be analogous to equation (2.3)). It is therefore difficult in general to study such a map by means other than numerical. We can however deduce the *linearized* form of the ANNNI map explicitly; this form will be useful in consideration of the stability of the map, in terms of its Lyapunov exponents [10].

We write $\mathcal{M}_d$ as

$$\begin{pmatrix} M_i \\ M_{i-1} \end{pmatrix} = \mathcal{M}_d \begin{pmatrix} M_{i-1} \\ M_{i-2} \end{pmatrix} = \begin{pmatrix} \text{implicit}(M_{i-1}, M_{i-2}) \\ M_{i-1} \end{pmatrix}. \tag{2.6}$$

Here the notation 'implicit(M_{i-1}, M_{i-2})' is the rule specified by equations (2.5) and (2.4). That is, M_i satisfies

$$0 = \frac{1}{2}g_T \ln\frac{1+M_i}{1-M_i} - 2g_0M_i - g_1M_{i-1} - g_2M_{i-2}. \tag{2.7}$$

Given fixed gs, and fixed M_{i-1} and M_{i-2}, this equation has either three solutions for M_i, or one. In the former case, there are two local minima of G (viewed as a function of the single variable M_i), bracketing a local maximum; the job of $\mathcal{M}_d$ is then to choose the lower of the two local minima. In the latter case the sole solution of (2.7) is a minimum. In either case we need an implicit solution of equation (2.7).

Implicit differentiation of (2.7) gives the linearized map

$$D\mathcal{M}_d = \begin{pmatrix} g_1/d & g_2/d \\ 1 & 0 \end{pmatrix} \tag{2.8}$$

where $d \equiv [g_T/(1-M_i^2)] - 2g_0$. The eigenvalues of the linearized map are then

$$\lambda_{1,2} = \frac{g_1 \pm \sqrt{g_1^2 + 4dg_2}}{2d} \tag{2.9}$$

and its determinant is

$$D \equiv \mathrm{Det}(D\mathcal{M}_d) = \lambda_1\lambda_2 = \frac{-g_2}{d}. \tag{2.10}$$

It is apparent that $|D|$ may be greater than or less than one. Fixed-point attractors of the map may be characterized by a single value for $|D|$, with $\lambda_1\lambda_2 < 1$, i.e., $\mu_1 + \mu_2 = \ln(\lambda_1) + \ln(\lambda_2) < 0$, where the μ_i are the Lyapunov characteristic exponents. For more complex attractors one can still define the Lyapunov exponents in terms of the long-time average shrinking and stretching behaviour of small volumes of phase space [10].

The map $\mathcal{M}_d$, defined above, may be viewed in two ways: as a dynamical system, with possible relevance to the problem of pattern formation [11] in open systems; or as a tool for the study of metastable states of the equilibrium problem represented by the free energy F. In this work, we will concentrate on the latter view. In order to apply the map $\mathcal{M}_d$ to the equilibrium problem, then, we need to relate attractors of the former to metastable states of the latter. This in turn necessitates relating the gs of G to the Js (here we implicitly include T) of F. In other words, given an attractor for a given set of gs, we want to view it as a likely metastable state of F, for some set of Js. The question is then, which Js?

As shown by Watson and Canright, the most useful strategy is not necessarily to set the gs equal to the corresponding Js (i.e., $g_T = T$, $g_1 = J_1$, etc). Instead, we assume that F has some 'simple' minima, and then attempt to design G (by constraining the gs in terms of the Js) so that, in the same range of Js where the simple minimum exists, G has an attractor which is identical to that minimum.

Specifically, we take the ferromagnetic state $M_i = \text{constant} = M$ as our simple, reference minimum of F. Whenever this state is metastable it will satisfy

$$\frac{\mathrm{d}F(\{M_i\} = M)}{\mathrm{d}M} = \frac{1}{2}T\ln\frac{1+M}{1-M} - 4J_0M - 2J_1M - 2J_2M = 0. \tag{2.11}$$

Since our map involves repeated minimization, every spin M_i satisfies (for any finite g_T)

$$\left.\frac{\partial G(x, M_{i-1}, M_{i-2})}{\partial x}\right|_{x=M_i} = 0. \tag{2.12}$$

(For $g_T = 0$, the minimum of G always occurs at one of the physical bounds ± 1 for the spin variables M_i. Hence equation (2.12) does not apply for this case. But for any finite value of g_T, one can show that the minimum always occurs between the two bounds, so equation (2.12) holds for each M_i.)

Now suppose that a ferromagnetic half-chain of spins ($M_\ell = M$, $\ell \leqslant i-1$) will produce, under the map $\mathcal{M}_d$, a new spin $M_i = M$, i.e., suppose that the ferromagnetic configuration is stable under the mapping. A necessary condition for this is that

$$\left.\frac{\mathrm{d}G}{\mathrm{d}M_i}\right|_{\{M_\ell\}=M_i=M} = \frac{1}{2}g_T\ln\frac{1+M}{1-M} - 2g_0M - g_1M - g_2M = 0. \tag{2.13}$$

Therefore, if we can enforce the equality of the right-hand sides of equations (2.11) and (2.13), we have ensured that a *necessary* condition for metastability of the 'simple' ferromagnetic state is equivalent to a *necessary* condition for mapping stability of the same state. That is, we have

$$(\text{FM is metastable}) \Longrightarrow (2.11) \iff (2.13) \Longleftarrow (\text{FM is mapping stable}). \tag{2.14}$$

Clearly this does *not* give (FM is metastable) $\iff$ (FM is mapping stable). However, this logic does give us some guidance in determining the gs of the map in terms of the Js

of the free energy—or, stated differently, guidance in choosing Js of the free energy from the gs of the map—such that attractors of the map, with the given gs, should be close to metastable states of F with the chosen Js.

Equating (2.11) to (2.13) does not uniquely determine the gs from the Js. For most of the present work, we took the obvious choice

$$T = g_T \qquad 2J_0 = g_0 \qquad 2J_1 = g_1 \qquad 2J_2 = g_2. \tag{2.15}$$

Given the above logic, however, we are not assured that attractors of the map are metastable states of F, with the correspondence given by equation (2.15). Therefore we find it necessary to test the metastability of any 'as-grown' configuration (attractor of the map), by relaxing it [8] to the nearest local minimum of the true free energy F. This last step can only be performed for a finite chain (typically of length 200); a standard numerical algorithm is used for this purpose. For the map to be most useful as a tool for studying the equilibrium problem, we expect that this last minimization step should make only small changes in the configuration given by the map. That is, in general, we ask that the attractors of the map be *close to* local minima of F.

3. Attractors of the map

The ANNNI problem is determined by four parameters; using one of these for our unit of energy leaves a three-dimensional parameter space. In line with the large majority of previous work [9], we take $J_0 = J_1 = 1$ in the following; this gives a two-dimensional phase diagram, which we view in the usual way in terms of the two coordinates $(\kappa, T/J_0)$. Here $\kappa = -J_2/J_1$, and we take $J_2 < 0$, $J_1 > 0$, hence studying only positive κ.

We first discuss some simple limiting cases. At $\kappa = 0$ the model is unfrustrated, with a continuous transition from ferromagnetic (FM) to paramagnetic (PM) at $T/J_0 = 6$. We find that the attractors of the map reproduce this line in the phase diagram perfectly. This is not surprising, since the map is designed, as much as possible, to give ferromagnetic minima of F as attractors—and, in mean-field theory, a paramagnetic chain is simply a ferromagnetic chain with $M = \text{constant} = 0$.

For finite κ, $0 < \kappa < 1/4$, the attractors of the map also reproduce perfectly the equilibrium phase diagram, including the correct values for $M(\kappa, T/J_0)$, and hence also the correct critical behaviour of M ($\propto (T_c - T)^{1/2}$) near the transition. We also find a *dynamic* critical behaviour at T_c, in that the largest Lyapunov exponent [10] μ_{max} at the fixed point goes to zero from below at T_c (or, more precisely, at $g_c = (g_T)_c = 2g_0 + g_1 + g_2$—which is the largest g_T for which equation (2.13) has a nonzero solution). In fact, since we can extract the small-M behaviour of the fixed point analytically from (2.13), we get that $\mu_{max} = -C_{\pm}|g_c - g_T|$, i.e., a linear vanishing of the Lyapunov exponent at g_c (with slope $C_{\pm}$ depending on the sign of $g_c - g_T$). We have verified this behaviour with simple numerical estimates of the largest Lyapunov exponent, near the FM and PM fixed points.

We next consider the line $T = 0$. Along this line, the equilibrium ANNNI problem shows a phase transition from the ferromagnet to a commensurate structure of period four (commonly termed $\langle 2 \rangle$ since it consists of spins of the form $\ldots + + - - + + - - \ldots$), at $\kappa = 1/2$. It is easily shown however that the FM is *metastable* (i.e., remains a local minimum of F) for any $\kappa < 1 + 2J_0/J_1$—that is, out to $\kappa = 3$, given the common convention $J_1 = J_0 = 1$. It is also easy to show that the FM attractor loses stability under the iterated mapping at $\kappa = 1$ [12]. Hence we find that the map $\mathcal{M}_d$, which we have 'trained' to find metastable FM states, does not have a FM attractor everywhere where there is a metastable FM state; nor does it always find the global minimum of F, even at $T = 0$. Instead, below

$\kappa = 1$, the map gives the (correctly) the metastable FM phase, while for $\kappa > 1$, the $\langle 2 \rangle$ configuration is both the attractor of the map, and the stable ground state.

It is implicit in the above that the map possesses a single attractor for the cases discussed. In fact, we find—as far as we can ascertain by numerical experiments—that the map $\mathcal{M}_d$ corresponding to the ANNNI problem possesses either a single attractor, or a pair of attractors related by spin inversion, for almost every choice [13] of $(g_T/g_0, g_2/g_1)$. This is in contrast to the results of Watson and Canright [8], and may be related to the lower dimensionality of the map in the present work (in that the number of *local* minima of our fictitious energy G is severely limited). With this simplifying feature, we can present a 'phase diagram' of attractors for the map.

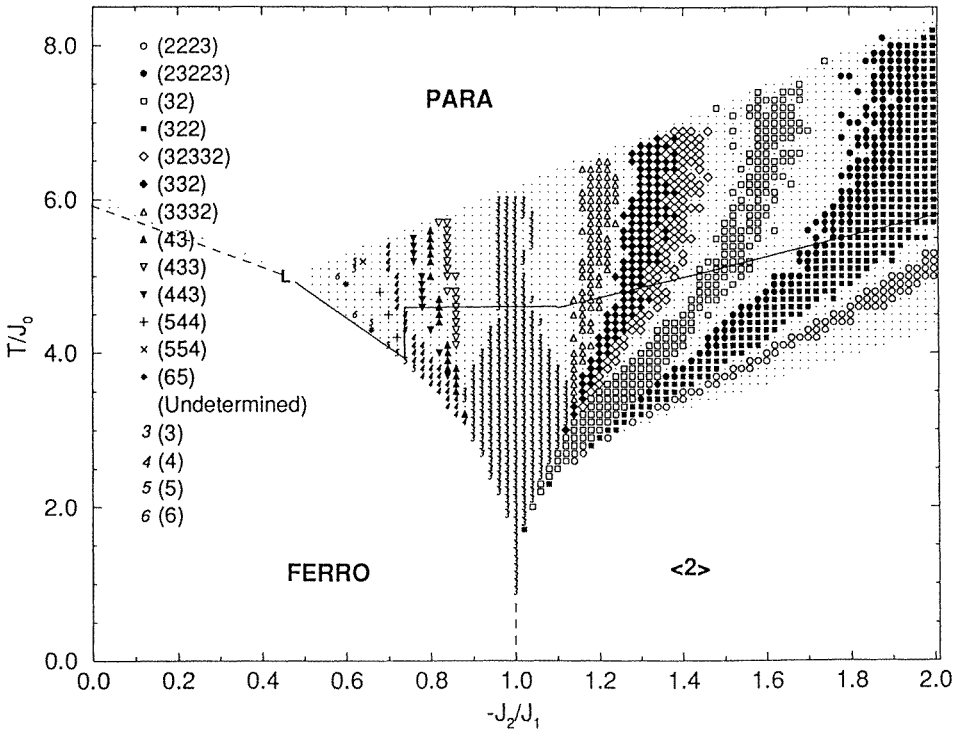

Figure 1. An attractor 'phase diagram' of the dissipative map. The coordinates of the 'phase diagram' are expressed in terms of the couplings of the ANNNI free energy. A variety of complex attractors are found over the parameter space; these attractors are then crudely (and approximately) sorted into the various categories of structure shown in the figure. Such structures are not necessarily periodic. Over most of the figure, the attractors of the map are close to, or equal to, local or global minima of the free energy. The exceptions are mainly found in the region between the paramagnetic phase and the thin solid line.

To obtain a crude sense of the attractor phase diagram, we scanned the rectangle $0 \leqslant g_T/g_0 \leqslant 4.25$, $0 \leqslant -g_2/g_1 \leqslant 2$—corresponding, via equation (2.15), to $0 \leqslant T/J_0 \leqslant 8.5$ and $0 \leqslant \kappa \leqslant 2$, as shown in figure 1. We then asked the computer to recognize a set of simple patterns [14] (as shown in the figure), based on the last 200 spins of an as-grown chain of 1000 spins. We emphasize that the patterns 'recognized' by the computer are not necessarily periodic; they simply obey the indicated sequence of sign changes over the 200

spins tested.

Remarkably, we find that the map $\mathcal{M}_d$, designed to closely mimic the equilibrium structures when they are 'simple', reproduces, qualitatively but in considerable detail, the phase diagram of the ANNNI problem. The shift of the multiphase point by a factor of two, described above, carries through to a rescaling of the entire phase diagram, along the κ-axis, by the same factor. Otherwise, the map's 'phase diagram' reproduces numerous detailed features of the ANNNI phase diagram: besides the above-mentioned ferromagnetic, paramagnetic, and $\langle 2 \rangle$ phases, there are other commensurate and incommensurate structures of various types.

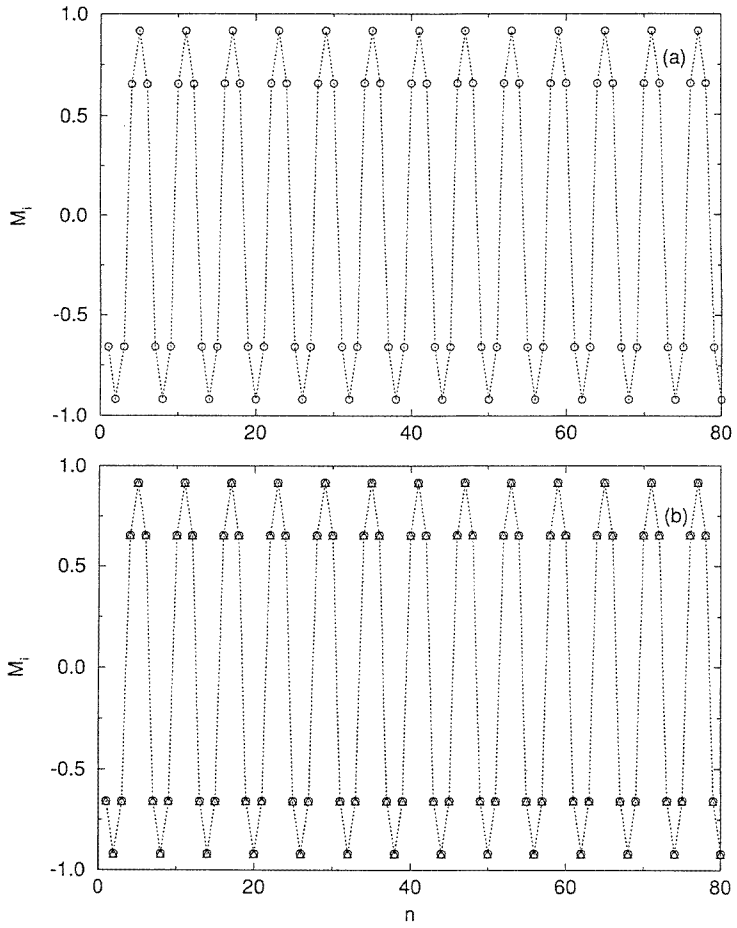

Figure 2. The commensurate structure at $(\kappa, T/J_0) = (1.0, 4.0)$. (a) The 'as-grown' attractor $\langle 3 \rangle$ of the map. (b) Comparison of the attractor (◯) with the nearest local minimum of the free energy (△), found by numerical relaxation.

Figure 2 shows a commensurate $\langle 3 \rangle$ structure at $(\kappa, T/J_0) = (1.0, 4.0)$. (Here and henceforth we always give parameters as Js, rather than gs, with the correspondence given by (2.15) implicit.) As noted in the previous section, after growing a chain, we discarded a few hundred layers from the chain and then relaxed the remaining finite configuration to the nearest local minimum of F. Figure 2(a) shows the as-grown chain, while 2(b) shows

superimposed both the as-grown and the relaxed chains. It is clear that our expectation that the attractor should be close to a metastable state of F is well met in this case, as it was for the simpler FM, $\langle 2 \rangle$, and paramagnetic structures. Comparing the two maps $\mathcal{M}_v$ and $\mathcal{M}_d$, we see that a period-six cyclic (unstable) trajectory of the former is closely matched by a period-six *attractor* of the latter.

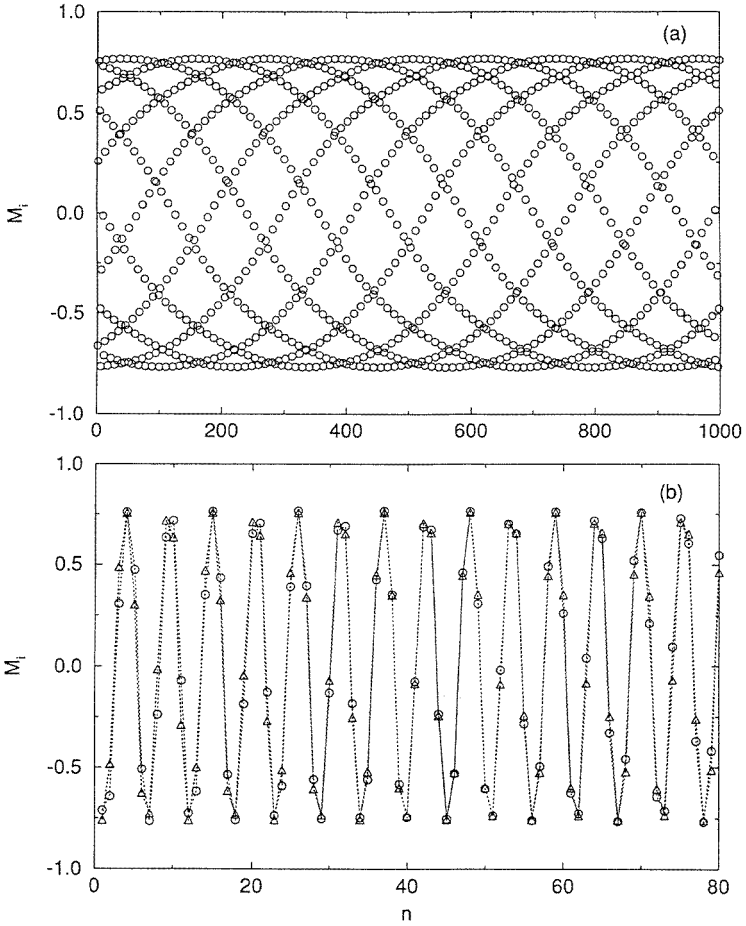

Figure 3. The unpinned incommensurate configuration at (1.2, 5.2). (a) The attractor. (b) Comparison of the attractor (◯) and the free-energy minimum (△)

An incommensurate structure at (1.2, 5.2) is shown in figure 3. Again we show the as-grown chain in figure 3(a) and compare the as-grown and relaxed chains in figure 3(b); and, again, the two are remarkably close. In particular, they have the same dominant wave vector. (Note that, even though this structure is incommensurate, it appears as a 'periodic' structure $\langle 3332 \rangle$ in our crude recognition procedure.) The close similarity seen in figure 3(b) means, again, that the two maps $\mathcal{M}_v$ and $\mathcal{M}_d$ have virtually identical closed, one-dimensional trajectories—one unstable, and one attracting.

We have observed the transition from the $\langle 2 \rangle$ 'phase' (attractor) at this same κ (=1.2), and lower T. We find that, at $T/J_0 = 2g_T/g_0 = T_{CC} \approx 2.803\,2806$, the $\langle 2 \rangle$ attractor loses stability to a $\langle 2^k 3 \rangle$ attractor (with k diverging at the transition). We thus find a

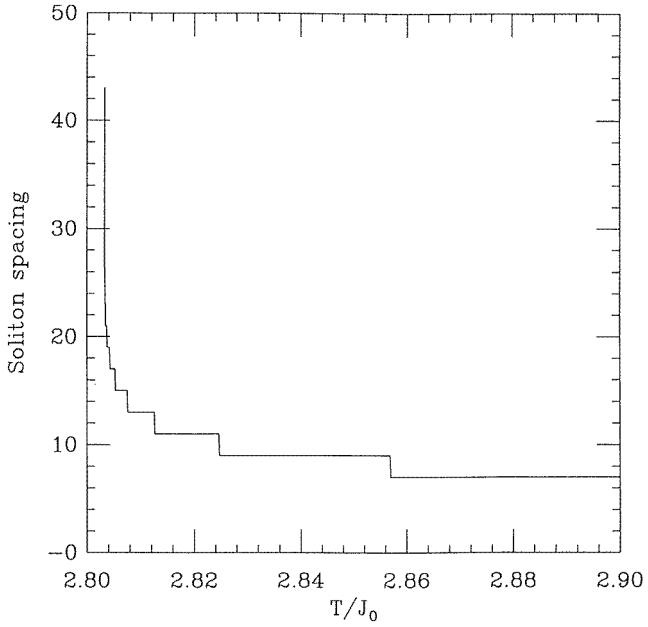

Figure 4. The intersoliton spacing, for solitons in a $\langle 2\rangle$ background, as a function of temperature T/J_0, at fixed $\kappa = 1.2$. The spacing diverges at a temperature $T_{CC} \approx 2.803\,2806$; below T_{CC} the solitons vanish, and the attractor is the simple $\langle 2\rangle$ structure. The displayed periodicities correspond to a $\langle 2^k 3\rangle$ structure for every integer k in the range $2 \leqslant k \leqslant 20$; we also found a '$k = 2.5$' attractor, that is, a $\langle 2^3 3 2^2 3\rangle$ structure, in the step (vertical to the eye) between the $\langle 2^3 3\rangle$ and $\langle 2^2 3\rangle$ attractors. We conjecture that the other steps shown may also be resolved into smaller steps, if viewed with finer resolution.

commensurate–commensurate transition, with the period of the attractor jumping from 4 to ∞ at T_{CC}. For $T \gtrsim T_{CC}$, k is finite (figure 4), and the attractor is simply the $\langle 2\rangle$ structure punctuated by a periodic array of solitons. In this range of T the solitons are pinned to the underlying lattice, so k is always an integer, and there are no incommensurate attractors. Incommensurate structures then occur at higher T, as the soliton density reaches a point at which intersoliton interactions depin them from the lattice. This picture is in qualitative agreement with that found by Høgh Jensen and Bak [1] for the equilibrium structures of the ANNNI problem: they found that, for κ sufficiently small (but above 0.5), the transition from the $\langle 2\rangle$ phase is to a pinned (commensurate) soliton lattice.

We also find some interesting differences from the equilibrium transition. For one thing, the $\langle 2\rangle$ attractor is asymmetric; that is, it takes the form $(a, a', -a, -a')$, while the equilibrium $\langle 2\rangle$ phase of F is of the symmetric form $(a, a, -a, -a)$. This asymmetry is very small at low T but becomes pronounced near the transition.

For the equilibrium ANNNI problem, at higher κ one expects [1] the effects of pinning to weaken, such that the transition from the $\langle 2\rangle$ phase is eventually directly into an incommensurate phase of unpinned (but still widely spaced) solitons. We have found a similar behaviour at higher κ—that is, a direct transition, at $T = T_{CI}$, from the commensurate $\langle 2\rangle$ attractor to an incommensurate attractor characterized by widely spaced solitons. Just above T_{CI} the attractor changes from period-four to a limit cycle. The orbit hence changes from four points at the corners of a rhombus to a one-dimensional

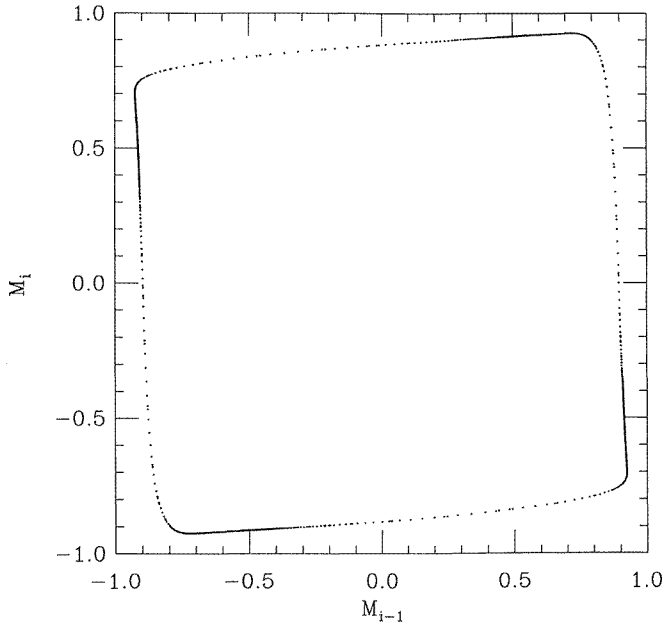

Figure 5. An orbit diagram of the attractor, just above the commensurate/incommensurate transition. Here we plot 20 000 points grown at (4.0, 7.7390). At this temperature the solitons are approximately 808 lattice spacings apart. This number is not exact because the solitons are incommensurate with the lattice; hence in the limit of an infinite chain, we expect the orbit to fill a one-dimensional curve.

(rhomboidal) curve, as shown in figure 5. In terms of the spin chain, there is an introduction of a soliton lattice for $T > T_{CI}$. In figure 6, we show one such soliton, grown near the commensurate/incommensurate transition at (4.0, 7.738 46). The spacing of these solitons, for $T > T_{CI}$ is, as far as we can resolve numerically, perfectly periodic. The structure is still incommensurate since the period is not fixed to integer values, instead varying smoothly with T. More quantitatively, we find that the period p of the solitons varies as $(T - T_{CI})^{-1/2}$.

There is a corresponding dynamical critical behaviour, as seen in the largest Lyapunov exponent μ_{max}. This quantity is of course negative for the stable $\langle 2 \rangle$ attractor, and is (presumably) zero for the incommensurate soliton lattice above T_{CI}. Our numerical estimates of μ_{max} give $\mu_{max} \propto (T_{CI} - T)^{1/2}$ on the low-T side of the transition. On the incommensurate side, it is difficult to obtain an accurate estimate for μ_{max}, since its *local* value varies widely along the attractor (positive in the solitons, negative in the flat $\langle 2 \rangle$ domains); however, our numerical estimates are consistent with zero, and hence with our belief that the incommensurate attractor has a one-dimensional orbit.

With increasing soliton density at higher T, the solitons begin to interact, giving a 'smoother' and more obviously incommensurate spin chain. At even higher density, the intersoliton interactions, combined with the soliton pinning energy, induce a transition to a high-period commensurate structure.

This sequence of transitions is very similar to that seen in the equilibrium ANNNI problem. It is also worth noting the differences. First, the solitons of the attractor are asymmetric; not surprisingly, when we relax such as-grown structures (figure 6(b)), the resulting soliton remains metastable, but is left–right symmetric (that is, symmetric with

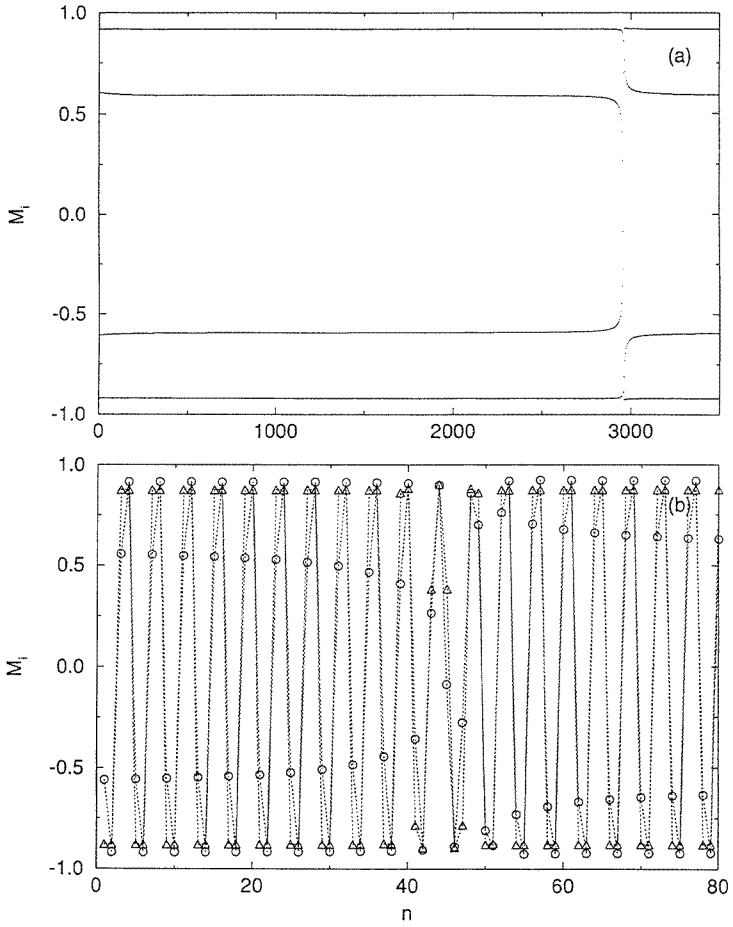

Figure 6. The soliton lattice at (4.0, 7.738 46). (a) Here we show only a piece of the attractor, in which the solitons are regularly spaced (spacing ~ 3051). (b) The relaxation of a small part of the as-grown chain, which includes the soliton (◯: as grown, △: relaxed).

respect to spatial inversion). We note further that a regime of widely spaced (hence noninteracting) but *periodic* solitons was not found by Høgh Jensen and Bak [1], using the area-preserving map $\mathcal{M}_v$. They noted that, in such a regime (pinning $\gg$ intersoliton repulsion), there should be a large number of nearly degenerate, metastable structures with irregular soliton spacing; hence they termed this regime 'chaotic'. Our mapping $\mathcal{M}_d$ however does not yield chaotic attractors in this regime. Instead, it picks out the single regular metastable structure in this huge, nearly degenerate set. There is no doubt that the periodic soliton lattice is also truly metastable; and it is plausibly the lowest- (free-) energy structure at the given soliton density. However, we agree with Høgh Jensen and Bak that, given the use of mean-field theory, and the tiny energy differences involved, it is physically reasonable to expect glassy rather than ordered behaviour in this regime.

In this sense figure 6 is both impressive and disappointing. It is remarkable that the simple map $\mathcal{M}_d$, designed to find ferromagnetic metastable states, has such a delicate structure as that of figure 6(a) as an attractor, and further that this attractor is very close

to a metastable minimum of the free energy F. Yet, since one of the principal reasons for interest in $\mathcal{M}_d$ was its promise for revealing chaotic (glassy) metastable structures, we find its failure to do so disappointing.

Of course, it is possible that $\mathcal{M}_d$ for the ANNNI problem has chaotic attractors which we failed to find. We can only say that we found none, in our crude search procedure (at parameter intervals 0.02 in each direction) represented by figure 1, and in a few high-resolution scans (such as that leading to figure 6(a)). Given our strong evidence that this simple two-dimensional map has, in almost all cases, a single attractor (or a pair of attractors related by spin inversion) for each parameter set, and given our failure to find any chaotic attractors, we conjecture that there are none for this map.

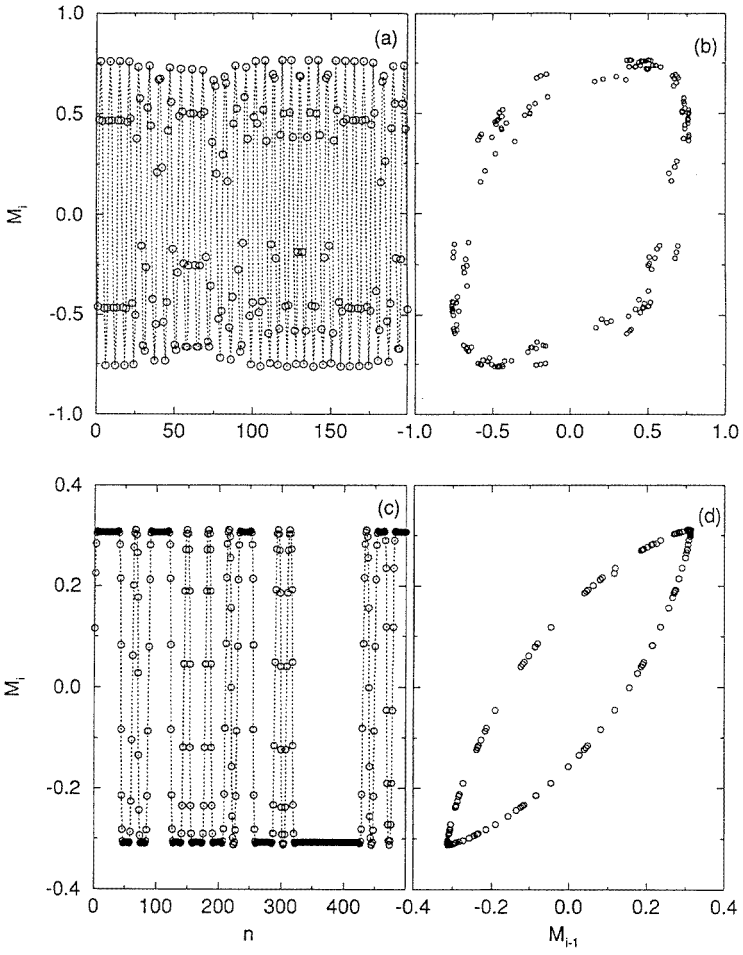

Figure 7. Two kinds of chaotic structure. (a) 'Strong' chaotic structure, found by relaxation from an incommensurate attractor at $(0.75, 4.7)$. (b) A phase portrait of the chaotic spin chain of (a). (c) 'Weak' chaotic structure, found by relaxation at $(0.21, 5.4)$ from a paramagnetic attractor. (d) A chase portrait of the chaotic spin sequence of (c).

We did find chaotic metastable structures for the ANNNI problem, but only by relaxing nonchaotic attractors. Two different kinds of chaotic structure are shown in figure 7.

In (a) and (b) we show a 'strong' chaotic structure—that is, one characterized by a highly irregular phase portrait in the (M_i, M_{i-1}) phase space (not to be confused with the $(T/J_0, \kappa)$ *parameter* space in which we view phase *diagrams*). The mapping gave an incommensurate chain—i.e., one whose phase portrait is a smooth, closed curve—when run at $(-g_2/g_1 = 0.75, g_T/g_0 = 2.35)$; when we relaxed this chain (at $(\kappa = 0.75, T/J_0 = 4.7)$, using our standard prescription), the smooth phase trajectory broke up as shown in figure 7(b): a chaotic structure was obtained. We have relaxed chains of 500 spins and higher, to verify that the structure we found was not simply an artifact of edge effects.

Obviously, this result represents a case for which the attractor and the nearest local minimum of F are (although not differing greatly in the overall phase portrait) *qualitatively* different—in contrast to the previous examples described above. There is in fact an entire region of the phase diagram (figure 1) in which this is commonly true. This region extends roughly from the solid line in figure 1 to the paramagnetic phase; it also (again, roughly) coincides with that region in the true phase diagram which is dominated by an infinity of incommensurate stable phases—most of which must have extremely small regions of stability (or metastability). Presumably, this is a partial explanation for the general failure of the map to find metastable structures in this region.

Another kind of chaotic state at $(0.21, 5.4)$ is shown in figures 7(c) and 7(d). Here the ('weak') chaos is more readily seen as a set of irregularly spaced defects in an underlying regular (ferromagnetic) structure; and the phase portrait of figure 7(d) is deceptively smooth, in contrast with that of figure 7(b). The structure shown was relaxed from a paramagnetic chain [15] at $(\kappa, T/J_0) = (0.21, 5.4)$, which is near the true Lifshitz point—but in the ferromagnetic region—of the equilibrium phase diagram.

The soliton (domain wall) density is clearly not small in figure 7(c), but the structure shown is nevertheless metastable. As we show in the next section, there are in most parts of the phase diagram an infinite number (more precisely, a number growing exponentially with the length N of the spin chain) of such metastable states. Essentially all of these metastable states are disordered, and yet, as we have seen, the attractors of our dissipative map $\mathcal{M}_d$ are invariably periodic or quasiperiodic—and they almost always 'point' to (are close to) a periodic or quasiperiodic metastable state.

4. Metastable states

In the previous section we have described in some detail the attractors of our map $\mathcal{M}_d$, and attempted to relate these attractors to metastable states of the mean-field ANNNI model. In order to put these results in context, it is of interest to study the set of metastable (MS) states for this problem—specifically, the number P of metastable states, and the density ρ of such states as a function of the free energy per spin f. In this section, we report some results for P and for $\rho(f)$ for the ANNNI problem.

The simplest case is that where $T > T_c$. Here there are no metastable states other than the PM phase. The proof is as follows.

A state $\{M_i\}$ is a local minimum of F if and only if $\partial F/\partial M_i = 0$ and the Hessian matrix $H_{ij} = \partial^2 F/\partial M_i\, \partial M_j$ is positive definite. Using (2.1), one finds

$$H_{i,i} = -4 + \frac{T}{1 - M_i^2} \qquad H_{i,i\pm1} = 1 \qquad H_{i,i\pm2} = -\kappa \tag{4.1}$$

and the condition $\partial F/\partial M_i = 0$ becomes

$$M_i + \alpha_i = \frac{T}{8} \ln \frac{1 + M_i}{1 - M_i} \tag{4.2}$$

where $\alpha_i \equiv \frac{1}{4}(M_{i-1} + M_{i+1}) - (\kappa/4)(M_{i-2} + M_{i+2})$ (and we again take $J_0 = J_1 = 1$ throughout this section). Since only the diagonal elements of the Hessian depend on the $\{M_i\}$, such that H_{ii} has an absolute minimum at $M_i = 0$, we conclude that, if $\{H_{ij}\}$ is positive definite for the PM phase when $M_i = 0$, then $\{H_{ij}\}$ is positive definite for *any* other set of spins $\{M_i\}$, at the same T. But a function with the Hessian matrix positive definite everywhere cannot have more than one extremum. This means that, for $T > T_c$, there are no metastable states other than the PM phase.

For $T < T_c$ the number of metastable states P will depend on the total number of spins N. We assume an exponential dependence

$$P(T, \kappa, N) = A(T, \kappa)a^N(T, \kappa). \tag{4.3}$$

In most cases we will restrict our consideration to finding a.

First, we consider the case where $T = 0$, when (2.1) reduces to

$$F(\{M_i\}, T = 0) = -2\sum_i M_i^2 - \frac{1}{2}\sum_i M_i((M_{i+1} + M_{i-1}) - \kappa(M_{i+2} + M_{i-2})). \tag{4.4}$$

To find local minima we will also need the dependence of $F(T = 0)$ on the single spin M_i, which is given by

$$F_0(M_i) = 2(-M_i^2 - 2\alpha_i M_i) \tag{4.5}$$

where α_i does not depend on M_i. Obviously, F_0, viewed as a function of the single variable M_i, is an inverted parabola, which achieves its local minima only at the boundaries, i.e. when $M_i = \pm 1$. This, in turn, means that the problem of finding minima of $F(\{M_i\}, T = 0)$ reduces to a selfconsistency problem for the $\{\alpha_i\}$. That is, $\{M_i\}$ is a local minimum of the free energy $F(\{M_i\})$, if and only if, for any i, $F_0(M_i)$ (given by (4.5)) is at a local minimum. Minima of $F_0(M_i)$ occur at: (i) $M_i = \pm 1$, if $|\alpha_i| < 1$; (ii) $M_i = +1$, if $\alpha_i \geqslant 1$; (iii) $M_i = -1$, if $\alpha_i \leqslant -1$. Requiring selfconsistency of these conditions then gives us the following criteria for metastable states at $T = 0$.

(1) $0 < \kappa < 1$, any sequence of ± 1 is metastable. The total number of metastable states is, obviously, 2^N.

(2) $1 < \kappa < 2$, any sequence of layers which does *not* have '111' in its Zhdanov representation [14] is metastable.

(3) $2 < \kappa < 3$, '111' and '$n1$', where $n \geqslant 3$, are prohibited.

(4) $\kappa > 3$, '111', '$n1$', $n \geqslant 3$, and '5' and greater are prohibited.

Given this set of rules, one can find the total number P of metastable states. One way to do this is to calculate numerically

$$a = \exp\left(\lim_{N\to\infty} \frac{\ln P(N, 0, \kappa)}{N}\right). \tag{4.6}$$

Alternatively, one can write a finite-difference equation for P (see below) which, when solved, yields a.

When $T > 0$, the coupled equations $\partial F/\partial M_i = 0$ cannot be solved analytically, but while $|M_i|$ is close to unity, one can use an approximate (perturbative) approach. If we suppose, for all i, that $M_i \approx M_i^0$, then $\alpha_i \approx \alpha_i^0$ (where the superscript 0 denotes the value of the variable at $T = 0$), and (4.2) becomes

$$M_i^0 + \alpha_i^0 \approx \frac{T}{8} M_i^0 \ln \frac{2}{1 - |M_i|}. \tag{4.7}$$

Here we have ignored terms of order $\delta_i = |M_i^0 - M_i| = 1 - |M_i|$. This gives

$$M_i \approx M_i^0\Big[1 - 2\exp(-8(1 + M_i^0\alpha_i^0)/T)\Big] \tag{4.8}$$

or $\delta_i = 2\exp(-8(1 + M_i^0\alpha_i^0)/T)$: that is, the mean-field layer magnetizations approach unity in magnitude very fast as $T \to 0$, as long as $M_i^0\alpha_i^0 > -1$. But for states which are metastable at $T = 0$ (see our criteria (i)–(iii) above), $M_i^0\alpha_i^0$ always exceeds -1, and so any metastable $T = 0$ state, continued to finite T using (4.8), represents a possible solution of (4.2) at finite T. If we consider the nonconstant (diagonal) elements of the Hessian matrix, which for low T are given by

$$H_{ii} = -4 + \frac{T}{4}\exp(8(1 + M_i^0\alpha_i^0)/T) \tag{4.9}$$

we see that $\lim_{T\to 0} H_{ii} = +\infty$, so H_{ii} is large and positive for some range of $T > 0$. Hence we conclude that a state metastable at $T = 0$ remains metastable over some finite range of T.

To estimate the temperature where the state disappears, we will use the following trick. A simple graphical analysis of (4.2) (i.e., LHS $\equiv f_L(M_i) = f_R(M_i) \equiv$ RHS) shows that three solutions (one unstable) become one solution, with increasing T, and that the lost MS state has (for at least one spin i) $M_i\alpha_i < 0$. Assuming that, until a state disappears in this way, $\alpha_i \approx \alpha_i^0$ for this spin, one gets

$$M_i + \alpha_i^0 = \frac{T}{8}\ln\frac{1 + M_i}{1 - M_i}. \tag{4.10}$$

Solutions of this equation will lose (meta)stability when

$$\frac{\partial f_R(M_i)}{\partial M_i} = \frac{T}{4(1 - M_i^2)} = +1$$

while simultaneously satisfying (4.10) and $M_i\alpha_i < 0$. These three conditions give an implicit equation for the temperature T at which a state disappears, which is

$$\alpha_i^0 = \frac{T}{8}\ln\frac{T}{4} - \frac{T}{4}\ln\left[1 + \left(1 - \frac{T}{4}\right)^{1/2}\right] + \left(1 - \frac{T}{4}\right)^{1/2} \equiv f(T). \tag{4.11}$$

However, there are only a few combinations of Zhdanov symbols for which $M_i\alpha_i < 0$, namely:

'111' disappears at $\frac{1}{2} + \kappa/2 = f(T)$
'11' disappears at $\frac{1}{2} = f(T)$
'1' disappears at $\frac{1}{2} - \kappa/2 = f(T)$ $(\kappa < 1)$
'n1' $(n \geqslant 3)$ disappears at $\kappa/2 = f(T)$
'n' $(n \geqslant 5)$ disappears at $\kappa/2 - \frac{1}{2} = f(T)$ $(\kappa > 1)$.

Using these relations, approximate boundaries where solutions containing these Zhdanov symbols disappear are shown in figure 8. We note that the last stability boundary listed above (i.e., that for all Zhdanov sequences including any symbol $n \geqslant 5$) should coincide with the stability boundary for the FM phase. We see from the figure that our approximation ($|M_i| \sim 1$) is quite good below $T/J_0 \approx 2$.

From the above, we can see that, even at finite (low) temperatures, the problem of counting metastable states reduces to the pure combinatoric problem of counting all possible combinations of allowed Zhdanov symbols. The last problem can be solved

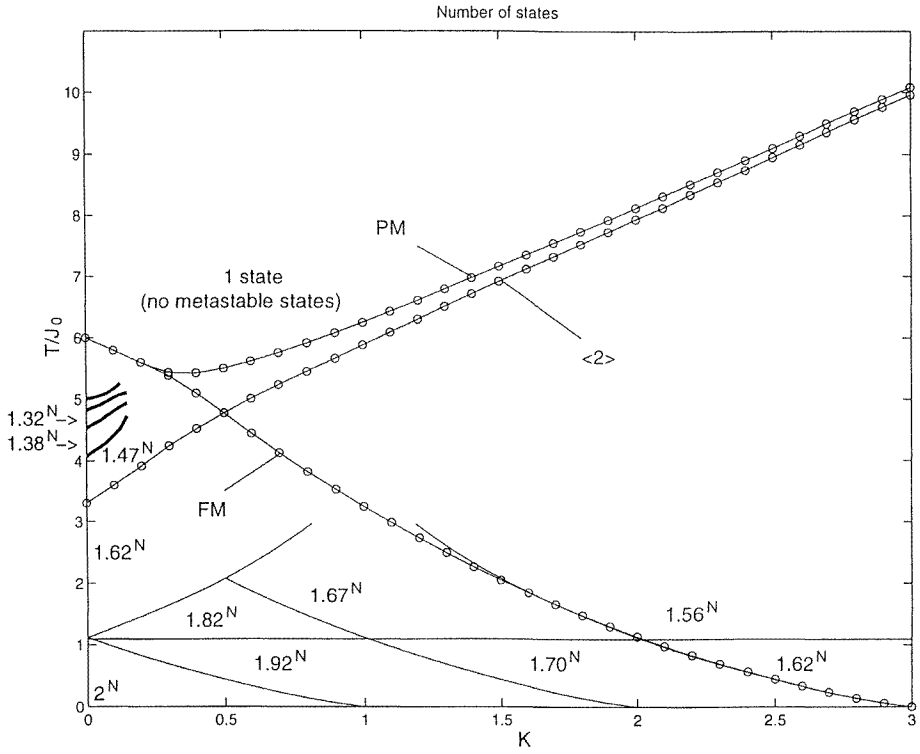

Figure 8. Approximate regions in the (κ, T) phase diagram for which we have counted the metastable states for the mean-field ANNNI problem. The leading exponential dependence of the number P of MS states is shown in each region. Lines with small circles represent the exact boundaries of *meta*stability for the PM, FM, and $\langle 2 \rangle$ phases, as indicated. The thin solid lines are obtained in the small-δ approximation, where $\delta_i = 1 - |M_i|$. The bold lines are obtained using a small-κ approximation (see the text).

either numerically, by calculating (4.6), or analytically. For instance, the number $P_1(N)$ of sequences of N spins which do *not* have '1' in their Zhdanov representation satisfies

$$P_1(N+1) = P_1(N) + P_1(N-1).$$

Assuming $P_1(N) = Aa^N$, one immediately gets the equation for a: $a = 1 + 1/a$ which corresponds to $a = 1.62$. In a similar fashion one can consider the other cases; the results are also presented in figure 8.

Another region where we were able to find (at least numerically) more or less clear-cut boundaries is the region of small κ ($\kappa \leqslant 0.15$). The reason for existence of the clear-cut boundaries in this region is that the interaction between spins is effectively restricted to the interaction between nearest neighbours. Therefore, spins in a given domain (where a domain is a sequence of spins between two successive changes of spin sign, that is, each Zhdanov symbol represents a domain) only 'feel' the domain boundaries—more specifically, the change of sign at the domain boundaries. This leads to the conclusion that for any given n, domains of length n will become unstable almost at the same T, for any MS state containing such domains. This conclusion was checked numerically in the following way. (1) A finite spin sequence (from 150–250 spins) of the form (Zhdanov sequence) 'LnL', where $L \gg n$, was constructed at $T = 0$. This structure was then 'tracked' with increasing T

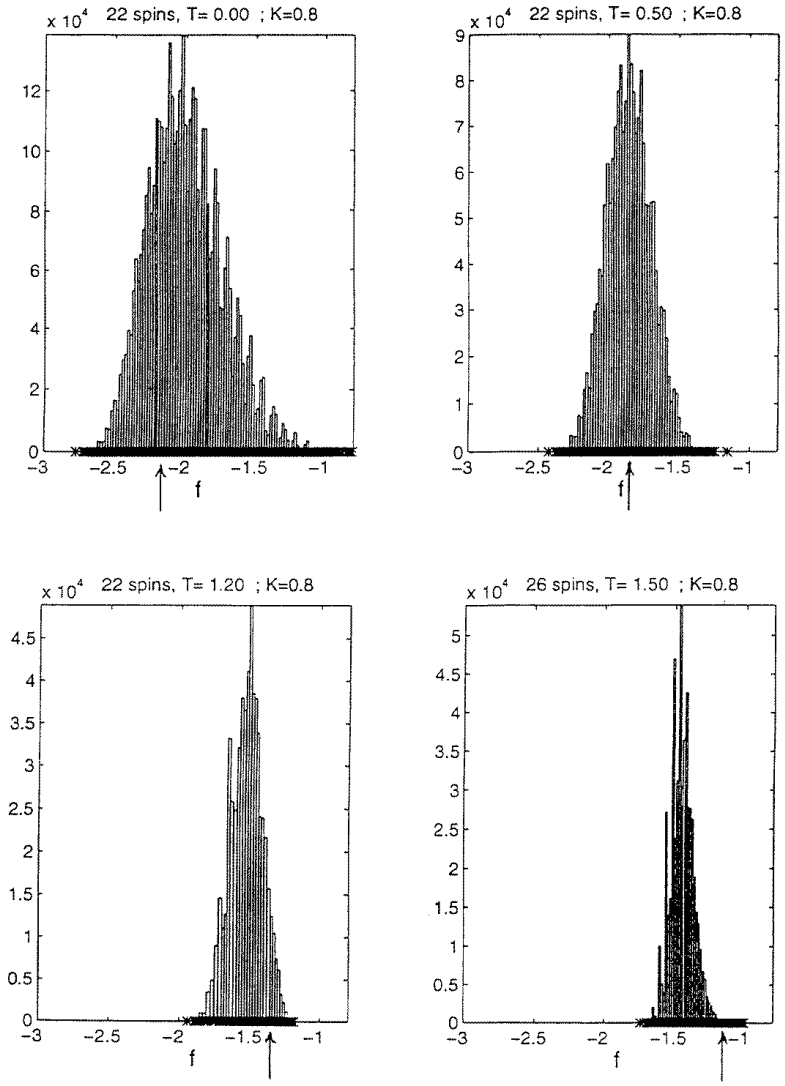

Figure 9. The distribution of metastable states in intensive free energy f, for several regions of figure 8. The energy of the FM state found by the map $\mathcal{M}_d$ is indicated by a small vertical arrow. Also, since some bars in the histogram are too small to see, every energy for which the number of MS states is nonzero is indicated by a '$\times$' on the abscissa.

by repeated relaxation after successive small increments δT (each time using the previously relaxed structure as the start state for the relaxation), until the n-domain disappeared at some $T_n^{(1)}$. (2) The same procedure was used, starting however with (a finite section of) the periodic structure $\langle n \rangle$ at $T = 0$; again the temperature was raised in small increments, each time relaxing the previous structure, until $\langle n \rangle$ became unstable and changed to some other structure at $T_n^{(2)}$. Usually this other structure still contained some domains of length n; hence the relaxation process was continued, with increasing T, until finally all domains of length n disappeared at some $T_n^{(3)}$. We did this numeric experiment for $n = 2$–6, and the result

(for κ small) was always the same: $T_n^{(1)} \leqslant T_n^{(2)} \leqslant T_n^{(3)}$, with $|T_n^{(1)} - T_n^{(3)}| \ll T_n^{(3)}$. Hence we can define some average temperature $T_n = (T_n^{(1)} + T_n^{(3)})/2$, and use this temperature as a good estimate of the point where domains of length n disappear. Repeating these calculations for different κ, we get the dependencies $T_n(\kappa)$. These dependencies are shown as bold lines on figure 8.

Another important question is the energy distribution of MS states. We did not attempt the general problem of finding the density of MS states $\rho(f)$; instead we restricted our consideration to the simpler case of low temperature (or more precisely, small δ_i: $|M_i| \sim 1$), where one can use the selection rules and perturbative expressions obtained above. We have used a simple approach: we exhaustively list all states which are allowed by the selection rules for a finite chain of fixed length, and plot the distribution of resulting intensive free energies. Our calculations show that the distribution obtained in this way is usually well-converged if our finite chain includes 20–25 spins. Figure 9 shows the distribution of MS states at a single $\kappa = 0.8$, for the four temperatures $T = 0, 0.5, 1.2, 1.5$, which correspond to four different regions of figure 8. To show the total range in energy, we have also marked the abscissa wherever the density of MS states is nonzero.

Watson and Canright [8] found that the map $\mathcal{M}_d$, applied to the flux-line problem, performed well in terms of locating low-energy MS states as attractors. In particular, the mapping was most successful where the problem (which had a tunable frustration) was highly frustrated, with a relatively large number of MS states. In figure 9 we show the corresponding performance of the current version of $\mathcal{M}_d$, applied to the ANNNI problem. Here we see the fact that the map possesses few attractors (essentially one) reflected in its relatively poor ability to single out low-energy MS states. For the indicated parameter values, the attractor is always ferromagnetic, while the equilibrium state (of minimal f) is the $\langle 2 \rangle$ phase. Of course, for $\kappa > 1$ $\mathcal{M}_d$ will give the lowest-energy structure. However, figure 9 makes the qualitative point that the relative inflexibility of $\mathcal{M}_d$ for this problem hampers its ability to find successfully low-energy metastable states.

5. Summary

In the present work we apply an idea of Watson and Canright [8], by writing a dissipative map $\mathcal{M}_d$ for the mean-field ANNNI problem which involves repeated minimization of a fictitious, asymmetric energy function. In contrast to the case studied by Watson and Canright, our problem gives a dissipative map whose dimension is fixed at two—i.e., at the (fixed) interaction range of the ANNNI problem. One (apparent) consequence of this simplification is that the map $\mathcal{M}_d$ possesses, in general, a single attractor (plus its spin-inverse) for a given set of parameters. Nevertheless, as shown in part in the figures, the map $\mathcal{M}_d$ displays a rich variety of attractors over the parameter space. These include ferromagnetic, paramagnetic, commensurate, and unpinned incommensurate structures, as well as pinned soliton lattices. Furthermore, the 'attractor phase diagram' (easily defined since there is essentially a single attractor for each parameter set) shows a remarkable qualitative similarity to the true phase diagram of the equilibrium problem. Hence our study adds to the growing body of evidence that nonlinear dynamical systems can present time-dependent behaviours with strong similarity to those static, spatially dependent structures exhibited by equilibrium systems.

If we further demand of our map that it reliably point to metastable structures of the corresponding equilibrium problem, we find somewhat mixed results. Over most of the phase diagram, the map succeeds in doing so. By 'most' we mean, at least roughly, wherever incommensurate phases are absent. It is not that the map cannot find metastable

incommensurate structures; it is rather that, in the region of the phase diagram in which such structures are prevalent, the map, more often than not, fails to find any qualitatively correct metastable structure. Of course, it is just in this region that the minima of the true free energy F are expected to be relatively weak, and to only exist over small regions of the phase diagram.

Somewhat surprisingly, the two-dimensional map $\mathcal{M}_d$ for the ANNNI problem apparently has no chaotic attractors anywhere in parameter space. There are good physical reasons to expect such structures for the mean-field ANNNI problem, and strong hints from earlier studies with a volume-preserving map that they should exist. We did find some (finite-size) examples of chaotic metastable structures, but only in the course of relaxing nonchaotic structures, generated by $\mathcal{M}_d$, to the nearest local minimum of the free energy F.

We believe that these glassy structures merit further study; they are in fact the *only* metastable structures of the ANNNI problem which have not yet yielded to systematic study. It seems however that the dissipative map idea, which was quite successful in finding chaotic states in the case studied by Watson and Canright, will not be useful here. We have here presented some limited results for the number and density (in free energy) of these disordered metastable states. We find an uncountable infinity of such states, in the limit $N \to \infty$, over the parts of the phase diagram studied (excluding of course the PM phase). Of this enormous variety of metastable states, it is somewhat remarkable that the dissipative map invariably finds the ordered (periodic or quasiperiodic) ones.

Finally, we note that the idea studied here still awaits a level of understanding which goes beyond numerical experiments. The present application represents a considerable simplification over the high-dimensional version of $\mathcal{M}_d$ studied by Watson and Canright. With this simplification, we have been able to obtain some limited analytical results for the dynamic critical behaviour of the map. However, we believe that further work is needed towards the goal of better understanding the behaviour and properties of this kind of dissipative dynamical system. One possible further simplification, which may merit investigation, is to make the map one-dimensional—which can still yield frustration, and hence complex behaviour, through the addition of an external potential (an example [2] is the Frenkel–Kontorova problem, which has an interaction range $r = 1$).

Acknowledgments

We thank Greg Watson, Julia Yeomans, Normand Mousseau, and David Sherrington for helpful discussions, and Normand Mousseau and David Sherrington for providing a preprint of their work. This work was supported in part by the NSF under Grant No DMR-9413057, and by the US Department of Energy through Contract No DE-AC05-84OR21400 with Martin Marietta Energy Systems Inc.

References

[1] Bak P 1981 *Phys. Rev. Lett* **46** 491; 1982 *Rep. Prog. Phys.* **45** 587
Høgh Jensen M and Bak P 1983 *Phys. Rev.* B **27** 6853

[2] Aubry S 1978 *Solitons and Condensed Matter Physics* ed A R Bishop and T Schneider (Berlin: Springer)
1983 *J. Physique* **44** 147; 1983 *Physica* D **7** 240; 1984 *Phys. Rep.* **103** 127
Aubry S and Le Daeron P Y 1983 *Physica* D **8** 381
Peyrard M and Aubry S 1983 *J. Phys. C: Solid State Phys.* **16** 1593

[3] Fisher M E and Huse D A 1981 *Melting, Localization, and Chaos* ed R K Kalia and P Vashishta (New York: North-Holland)

[4] Fradkin E, Hernandez O, Huberman B A and Pandit R 1983 *Nucl. Phys.* B **215** [FS7] 137

[5] Janssen T and Tjon J A 1983 *J. Phys. C: Solid State Phys.* **16** 4789; 1983 *J. Phys. A: Math. Gen.* **16** 673
[6] Pandit R and Wortis M 1982 *Phys. Rev.* B **25** 3226
Legrand B, Tréglia G and Ducastelle F 1990 *Phys. Rev.* B **41** 4422
Tréglia G, Legrand B, Eugène J, Aufray B and Cabané F 1991 *Phys. Rev.* B **44** 5842
Trallori L, Politi P, Rettori A, Pini M G and Villain J 1994 *Phys. Rev. Lett.* **72** 1925
[7] This property can be shown to hold for any 1D problem which satisfies the detailed-balance conditions $J_{ij} = J_{ji}$. See [1–6] for examples.
[8] Watson G I and Canright G S 1993 *Phys. Rev.* B **48** 15 950
Canright G S and Watson G I 1994 *Computer Simulation Studies in Condensed-Matter Physics VII* ed D P Landau, K K Mon and H-B Schüttler (Berlin: Springer) p 204
[9] The ANNNI model has been studied by many workers. See, for example,
Elliott R J 1961 *Phys. Rev.* **124** 346
Selke W 1984 *Modulated Structure Materials* ed T Tsakalakos (Boston, MA: Martinus Nijhoff)
Yeomans J 1988 *Solid State Physics* ed H Ehrenreich and D Turnbull (San Diego, CA: Academic)
Fisher M E and Selke W 1980 *Phys. Rev. Lett.* **44** 1502
and [1].
[10] Schuster H G 1988 *Deterministic Chaos* (Weinheim: VCH)
[11] The idea of an iterated minimization process as a dissipative map has been recently applied with great success to the problem of pattern formation in plants. See
Douady S and Couder Y 1992 *Phys. Rev. Lett.* **68** 2098
[12] Our map $\mathcal{M}_d$, at $T = 0$, is in fact a special case of a dynamical (but 'temperature'-dependent) rule studied by
Mousseau N and Sherrington D 1996 *Preprint*
in the limit of complete asymmetry (and $T = 0$)—for which they find the same stability limit.
[13] We found an example of multiple attractors, unrelated by symmetry, at $g_T/g_0 = 1.8$, $-g_2/g_1 = 0.8$. Here the attractors are two FM structures (+ and −) and a $\langle 4 \rangle$ structure. These multiple attractors persist only over a narrow range of parameters; this range defines a 'phase boundary' between the FM and $\langle 4 \rangle$ 'phases'. Conceivably, all of our 'phase boundaries' (cf. figure 1) have this property; but if so, the parameter range for multiple attractors is quite small. For this specific case, we examined the basin boundaries numerically. They show no sign of fractal geometry and hence give no sign of a chaotic repellor.
[14] Any set of 'spins' $\{M_i\}$, $|M_i| \leqslant 1$, may be described (with some loss of information) in terms of the sequence of *signs* $M_i/|M_i|$, or even more concisely by a set of integers giving the number of adjacent repetitions of the same sign. For example, the periodic sequence $\cdots - - + + - - + + - - + + - - \cdots$ is denoted by the Zhdanov symbol $\langle 2 \rangle$. In this paper, we have broadened the usage to include nonperiodic strings. See, for example, the work of Julia Yeomans cited in [9] and
Zhdanov G S 1945 *C. R. Acad. Sci. URSS* **48** 43
[15] The unrelaxed (paramagnetic) chain was grown by the map at $(-g_2/g_1, g_T/g_0) = (0, 42, 2.7)$. That is, we relaxed at $\kappa = (1/2)(-g_2/g_1)$ rather than the prescription $\kappa = -g_2/g_1$ obtained from the relations in equation (2.15) We performed a number of relaxations using this modified prescription, motivated by the obvious rescaling of the abscissa seen in the attractor phase diagram. The results, in terms of accuracy of the map in finding metastable structures, were not significantly better than those obtained by the usual prescription.